THE RADIATION FIELD PRODUCED BY AN INFINITE SLOT IN AN INFINITE CYLINDER SURROUNDED BY A HOMOGENEOUS PLASMA SHEATH

DIPAK L. SENGUPTA

RADAR LABORATORY
Institute of Science and Technology
THE UNIVERSITY OF MICHIGAN

May 1963

Contract AF 33(616)-8365

4563-35-T

THE RADIATION FIELD PRODUCED BY AN INFINITE SLOT IN AN INFINITE CYLINDER SURROUNDED BY A HOMOGENEOUS PLASMA SHEATH

DIPAK L. SENGUPTA

May 1963

Radar Laboratory
Institute of Science and Technology
THE UNIVERSITY OF MICHIGAN
Ann Arbor, Michigan

4563-35-T

THE RADIATION FIELD PRODUCED BY AN INFINITE SLOT IN AN INFINITE CYLINDER SURROUNDED BY A HOMOGENEOUS PLASMA SHEATH

DIPAK L. SENGUPTA

May 1963

Radar Laboratory
Institute of Science and Technology
THE UNIVERSITY OF MICHIGAN
Ann Arbor, Michigan

NOTICES

Sponsorship. The work reported herein was conducted by the Institute of Science and Technology for the U. S. Air Force, Contract AF 33(616)-8365. Contracts and grants to The University of Michigan for the support of sponsored research by the Institute of Science and Technology are administered through the Office of the Vice-President for Research.

Acknowledgments. The author would like to express his thanks to Mr. R. E. Hiatt for correcting the manuscript, and to Mr. H. Hunter and Mr. D. R. Hodgins for carrying out the numerical computations.

ASTIA Availability. Qualified requesters may obtain copies of this document from:

Armed Services Technical Information Agency
Arlington Hall Station
Arlington 12, Virginia

Final Disposition. After this document has served its purpose, it may be destroyed. Please do not return it to the Institute of Science and Technology.

CONTENTS

FIGURES

TABLES

THE RADIATION FIELD PRODUCED BY AN INFINITE SLOT IN AN INFINITE CYLINDER SURROUNDED BY A HOMOGENEOUS PLASMA SHEATH

ABSTRACT

The radiation properties of a slotted cylindrical antenna surrounded by a homogeneous plasma sheath have been investigated. The slot is axial and extends along the entire length of the cylinder; it is fed by a voltage of constant magnitude and phase. The antenna is insulated from the plasma by a thin dielectric coating.

General expressions for the field components are derived, and then simplified by making some physical approximations. The radiation patterns produced by the antenna are discussed for the following two cases: (i) when both the dielectric coating and the plasma sheath are thin, and (ii) when only the dielectric coating is thin. For both cases field expressions are derived for operating frequency above the plasma frequency and below it. The effects of collision between the particles in the plasma are taken into account. Results for the collisionless case can be obtained from the general expressions given. Numerical results are obtained for the radiation patterns produced by the antenna under various physical situations.

1
INTRODUCTION

This report investigates the radiation field produced by a thin longitudinal slot in an infinitely long conducting cylinder surrounded by a homogeneous plasma sheath. Figure 1 shows schematically a section of a cylinder of radius a with a longitudinal slot of angular width ϕ_o. It is assumed that the slot is very thin and that it is fed between its edges with a voltage which is uniform in magnitude and phase along the length of the slot; the slot being very thin, the exciting field can be assumed to be uniform in magnitude and phase across the transverse dimension of the slot. The antenna should be provided with an insulating cover in the immediate vicinity of the feed so that the assumed voltage or current distribution will be realized and any conduction losses in the ionized medium will not be excessive. In the present investigation the slot is assumed to be insulated from the plasma sheath by a thin coating of a dielectric material. The positions of the different media with respect to the slotted cylinder are shown schematically in Figure 2.

Except for the presence of the plasma sheath, the investigation reported herein is a standard boundary value problem which was solved many years ago [1, 2]. Wait [2] has analyzed in detail the problem of a finite slot in a conducting cylinder of infinite length and covered with a thin

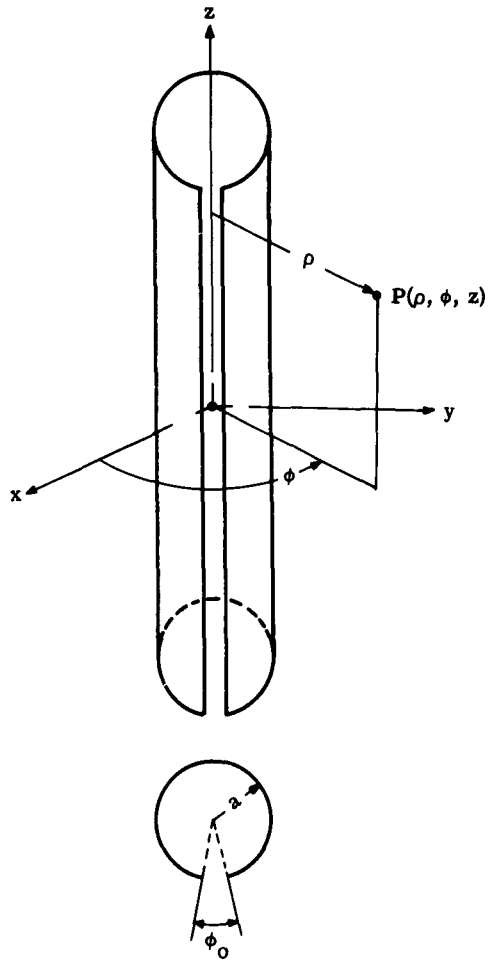

FIGURE 1. A SECTION OF AN INFINITELY LONG SLOTTED CYLINDER. The coordinate system is also shown.

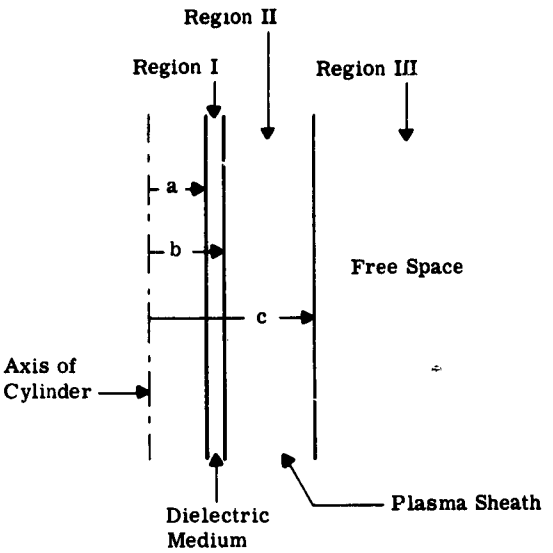

FIGURE 2. THE ORIENTATION OF DIFFERENT MEDIA

dielectric coating. In principle, one can similarly analyze a finite slot in a dielectric covered infinite cylinder surrounded by a plasma sheath. However, the results of such an analysis become extremely complicated, and it is not easy to arrive at useful conclusions without making elaborate machine calculation. In a recent report [3] Rusch extended Wait's work to the case of a finite slot in a cylinder covered with a homogeneous and lossless plasma. The present investigation differs in that we assume that the plasma is lossy and that the slot is insulated from the plasma by a dielectric coating. The presence of the dielectric coating makes the problem more complicated. Hodara too has studied a similar problem [4], which differs from the present one in that he deals with the radiation from a magnetic line source supported by a perfectly conducting plane and coated with a sheath of lossy gyro-plasma.

The infinite slot case to be considered here is a two-dimensional problem; consequently it is relatively easy to handle analytically and, as we shall see later, some of the results can be directly applied to the more important case of a finite slot. Even though the infinitely long slot is unrealistic from the practical point of view, investigation of the radiation pattern it produces has great practical value because it gives the principal plane pattern (azimuthal or x-y plane in Figure 1) of a similarly excited finite slot in a cylinder [1].

It is well known that, in the absence of a steady magnetic field, a low-density plasma can be represented by a homogeneous dielectric medium having an equivalent permittivity which is sensitive to the operating frequency and which depends on the physical parameters of the plasma, e.g., on the plasma frequency ω_p and the collision frequency ν. In general, the equivalent permittivity is a complex quantity; it reduces to a real quantity when the plasma is collisionless or the collision effects are negligible. For operating frequencies $\omega >> \omega_p$ the equivalent permittivity of the plasma may be assumed to be equal to that of free space, in which case the antenna's performance should not be influenced by the presence of the plasma sheath. For $\omega < \omega_p$, the plasma sheath becomes opaque to the electromagnetic waves and the sheath behaves like a conducting medium, thus attenuating the electromagnetic waves passing through. We intend to investigate the radiation pattern produced by the infinite slot for both $\omega > \omega_p$ and $\omega < \omega_p$.

The present problem is important in connection with the performance of an antenna in a space vehicle re-entering the atmosphere or moving through an ionized region in space. At the time of re-entry the space vehicle is surrounded by a plasma sheath with a high density of charged particles; the resulting plasma frequency may be high compared to the operating frequency of the antenna. Depending on the relative difference between the operating frequency and the plasma frequency, during re-entry the radio communication from the space vehicle may or may not be lost momentarily. It is hoped that the present analysis will shed some light on this phenomenon, and also on the influence of the various physical parameters of the plasma on the radiation pattern produced by the antenna.

The scheme of the report is as follows. At first the problem is formulated in general terms so that the theory can be applied to homogeneous plasma sheaths as well as inhomogeneous ones. The theory is then applied to the homogeneous sheath. Exact expressions for the field components are derived. The general expressions are then simplified by making various physical approximations. The approximations are divided into two broad categories: (i) when both the dielectric coating and the plasma sheath are thin and (ii) when only the dielectric coating is thin. In both cases we give general expressions for $\omega > \omega_p$ and $\omega < \omega_p$. The effects of collision are also discussed in detail. In all cases it is assumed at first that the antenna is covered with a thin dielectric coating. Later, we make the approximation that the effect of the thin dielectric coating on the radiation field is negligible compared to that of the plasma; this simplifies the expressions considerably. The final section of the report gives the results of numerical calculations. The radiation patterns given under various physical situations bring out the influence of the plasma sheath on the performance of the antenna. The values of the different parameters chosen for computation may or may not be typical for practical cases; they have been chosen here partly for ease of computation.

2
FORMULATION OF THE PROBLEM

In this section we solve the source-free Maxwell's equations in the different media and then determine the general expressions for the fields. These expressions are obtained in the form of infinite series with unknown coefficients. The exciting field is then expressed as a Fourier series. The unknown coefficients in all the expressions are determined after applying the relevant boundary conditions to the fields at the interface between the various media [5, 6].

If we start from Maxwell's equations and assume in general that the permittivity ϵ and permeability μ of the medium are inhomogeneous in space, it can be shown that the magnetic and electric fields satisfy the following two vector equations:

$$\nabla \cdot \nabla \vec{H} + \omega^2 \mu\epsilon \vec{H} + \nabla\left(\frac{\vec{H} \cdot \nabla \mu}{\mu}\right) + i\omega \nabla\epsilon \times \vec{E} = 0 \tag{1}$$

$$\nabla \cdot \nabla \vec{E} + \omega^2 \mu\epsilon \vec{E} + \nabla\left(\frac{\vec{E} \cdot \nabla \epsilon}{\epsilon}\right) - i\omega \nabla\mu \times \vec{H} = 0 \tag{2}$$

where ∇ is the gradient operator

ω is the operating frequency in radians

the assumed time dependence is $e^{i\omega t}$

In the present problem the permittivity ϵ is assumed to be a function of the radial distance ρ only, and the permeability μ is assumed to be constant so that $\nabla\mu = 0$. Because of the two-dimensional nature of the problem and the assumed type of excitation of the slot, the field quantities will not vary in the z-direction; also there will be a component E_ϕ of the electric field and perhaps an E_ρ, but no E_z. For the present problem, therefore, it is sufficient to solve the following equation for H_z obtained from Equation 1 under the above assumptions:

$$\nabla^2 H_z + \omega^2 \mu\epsilon H_z - \frac{1}{\epsilon}\frac{\partial \epsilon}{\partial \rho}\frac{\partial H_z}{\partial \rho} = 0 \tag{3}$$

where we have used cylindrical coordinates (ρ, ϕ, z). It can be shown that under these circumstances $H_\rho = H_\phi = 0$ and that all the other field components can be expressed in terms of the axial components H_z of the magnetic field. Thus we obtain

$$E_\rho = \frac{1}{i\omega\epsilon\rho}\frac{\partial H_z}{\partial \phi} \tag{4}$$

$$E_\phi = \frac{1}{i\omega\epsilon}\frac{\partial H_z}{\partial \rho} \tag{5}$$

Equation 3 is an inhomogeneous partial differential equation of the second order. It is not possible to solve this equation for general variation of ϵ; but various exact and approximate methods have been developed for some special types of variation of ϵ [7, Chapter 4]. Since we are interested in the homogeneous case only (ϵ is a constant), we need not go into these details.

2.1. EXPRESSIONS FOR THE FIELD COMPONENTS

In this section we derive the field expressions for the homogeneous plasma sheath. The plasma sheath is replaced by a homogeneous medium with an equivalent permittivity. In Section 2.2 we will discuss further the nature and value of this permittivity. As shown in Figure 2, we divide the medium into three distinct homogeneous regions and obtain explicit expressions for the fields in these regions. The field expressions are obtained after solving the homogeneous Helmholtz equation, obtained from Equation 3 after assuming ϵ to be constant in space in each of the three regions. The general expressions for the fields in the different regions are as follows:

Region I. $a \leq \rho \leq b$, the region consisting of the dielectric coating:

$$H_z^{I} = \sum_{n=-\infty}^{\infty} \left[a_n H_n^{(1)}(\beta_1\rho) + b_n H_n^{(2)}(\beta_1\rho)\right] e^{in\phi} \tag{6}$$

$$E_\phi^{I} = \frac{i\beta_1}{\omega\epsilon_1} \sum_{n=-\infty}^{\infty} \left[a_n H_n^{(1)'}(\beta_1\rho) + b_n H_n^{(2)'}(\beta_1\rho)\right] e^{in\phi} \tag{7}$$

Region II. $b \leq \rho \leq c$, the plasma sheath region:

$$H_z^{II} = \sum_{n=-\infty}^{\infty} \left[A_n H_n^{(1)}(\beta_2\rho) + B_n H_n^{(2)}(\beta_2\rho)\right] e^{in\phi} \tag{8}$$

$$E_\phi^{II} = \frac{i\beta_2}{\omega\epsilon_2} \sum_{n=-\infty}^{\infty} \left[A_n H_n^{(1)'}(\beta_2\rho) + B_n H_n^{(2)'}(\beta_2\rho)\right] e^{in\phi} \tag{9}$$

Region III. $c \leq \rho \leq \infty$, the free-space region:

$$H_z^{III} = \sum_{n=-\infty}^{\infty} D_n H_n^{(2)}(\beta_3\rho) e^{in\phi} \tag{10}$$

$$E_\phi^{III} = \frac{i\beta_3}{\omega\epsilon_3} \sum_{n=-\infty}^{\infty} D_n H_n^{(2)'}(\beta_3\rho) e^{in\phi} \tag{11}$$

where $\beta_1 = \omega(\mu_o \epsilon_1)^{1/2}$, $\beta_2 = \omega(\mu_o \epsilon_2)^{1/2}$, $\beta_3 = \omega(\mu_o \epsilon_3)^{1/2}$ are the propagation constants of the dielectric coating, the plasma sheath, and free space, respectively (ϵ_1, ϵ_2, ϵ_3 are the permittivities of the three regions, respectively)

μ_o is the permeability, assumed to be the same for all three media

a_n, b_n, A_n, B_n, and D_n are five unknown coefficients to be determined shortly

H_n is the standard notation for Hankel functions

' indicates differentiation with respect to the total argument of the Hankel functions

The tangential electric field in the infinite slot will in general have a ϕ-component which we consider a prescribed function $f_1(\phi)$. In view of the infinite conductivity of the wall, this function represents a complete knowledge of the tangential electric field over the entire surface of the cylinder, namely,

$$\left.\begin{aligned} E_\phi &= f_1(\phi) \qquad \text{for } -\frac{\phi_o}{2} \le \phi \le \frac{\phi_o}{2} \\ &= 0 \qquad \text{outside the slot} \end{aligned}\right\} \tag{12}$$

We now develop the Fourier expansion for the tangential components of the electric field over the surface of the cylinder. In the ϕ-direction E_ϕ is a periodic function and is therefore expressed by a Fourier series,

$$E_\phi(\phi) = \sum_{n=-\infty}^{\infty} T_n e^{in\phi} \tag{13}$$

where

$$T_n = \frac{1}{2\pi} \int_{-\phi_o/2}^{\phi_o/2} f_1(\xi) e^{-in\xi} d\xi \tag{14}$$

In the present case the slot is uniformly excited, and we assume that $f_1(\phi) = E_o$ in Equation 12. Thus, after substituting Equation 12 in Equation 14 and carrying out the integration, we obtain the following for the tangential component of the electric field over the surface of the cylinder:

$$E_\phi = \sum_{n=-\infty}^{\infty} \frac{E_o}{n\pi} \sin\left(\frac{n\phi_o}{2}\right) e^{in\phi} \tag{15}$$

Now, applying the boundary condition that the tangential components of the electric and magnetic fields are continuous at the interface between two media, we obtain the following five equations for the five unknown coefficients:

$$a_n H_n^{(1)'}(\beta_1 a) + b_n H_n^{(2)'}(\beta_1 a) = \frac{\omega\epsilon_1}{i\beta_1}\frac{E_o}{n\pi}\sin\left(\frac{n\phi_o}{2}\right) \tag{16}$$

$$a_n H_n^{(1)}(\beta_1 b) + b_n H_n^{(2)}(\beta_1 b) = A_n H_n^{(1)}(\beta_2 b) + B_n H_n^{(2)}(\beta_2 b) \tag{17}$$

$$a_n\beta_1\epsilon_2 H_n^{(1)'}(\beta_1 b) + b_n\beta_1\epsilon_2 H_n^{(2)'}(\beta_1 b) = A_n\beta_2\epsilon_1 H_n^{(1)'}(\beta_2 b) + B_n\beta_2\epsilon_1 H_n^{(2)'}(\beta_2 b) \tag{18}$$

$$A_n H_n^{(1)}(\beta_2 c) + B_n H_n^{(2)}(\beta_2 c) = D_n H_n^{(2)}(\beta_3 c) \tag{19}$$

$$A_n\beta_1\epsilon_3 H_n^{(1)'}(\beta_2 c) + B_n\beta_2\epsilon_3 H_n^{(2)}(\beta_2 c) = D_n\beta_3\epsilon_2 H_n^{(2)'}(\beta_3 c) \tag{20}$$

In order to evaluate the unknown coefficients from Equations 16 through 20 we need to evaluate the following determinant:

$$D = \begin{vmatrix} H_n^{(1)'}(\beta_1 a) & H_n^{(2)'}(\beta_1 a) & 0 & 0 & 0 \\ H_n^{(1)}(\beta_1 b) & H_n^{(2)}(\beta_1 b) & -H_n^{(1)}(\beta_2 b) & -H_n^{(2)}(\beta_2 b) & 0 \\ \beta_1\epsilon_2 H_n^{(1)'} & (\beta_1 b)\beta_1\epsilon_2 H_n^{(2)'}(\beta_1 b) & -\beta_2\epsilon_1 H_n^{(1)'}(\beta_2 b) & -\beta_2\epsilon_1 H_n^{(2)'}(\beta_2 b) & 0 \\ 0 & 0 & H_n^{(1)}(\beta_2 c) & H_n^{(2)}(\beta_2 c) & -H_n^{(2)}(\beta_3 c) \\ 0 & 0 & \beta_2\epsilon_3 H_n^{(1)'}(\beta_2 c) & \beta_2\epsilon_3 H_n^{(2)'}(\beta_2 c) & -\beta_3\epsilon_2 H_n^{(2)'}(\beta_3 c) \end{vmatrix} \tag{21}$$

Since we are interested in the radiation field only, we evaluate the coefficient D_n. It can be shown that D_n is given by

$$D_n = D'/D \tag{22}$$

where D' is the determinant obtained from Equation 21 after replacing the terms in its last column by (P, 0, 0, 0, 0), where $P = \frac{\omega\epsilon_1}{i\beta_1}\frac{E_o}{n\pi}\sin\frac{n\phi_o}{2}$. After expanding the determinant D as given by Equation 21, the following is obtained,

$$D = L_n\left[\beta_2\beta_3\epsilon_1\epsilon_2 H_n^{(2)'}(\beta_3 c)M_n + \beta_2^{\,2}\epsilon_1\epsilon_3 H_n^{(2)}(\beta_3 c)N_n\right]$$

$$+ \beta_1\epsilon_2 P_n\left[\beta_3\epsilon_2 H_n^{(2)'}(\beta_3 c)Q_n + \beta_2\epsilon_3 H_n^{(2)}(\beta_3 c)R_n\right] \tag{23}$$

where

$$\left.\begin{aligned}
L_n &= H_n^{(1)'}(\beta_1 a)H_n^{(2)}(\beta_1 b) - H_n^{(1)}(\beta_1 b)H_n^{(2)'}(\beta_1 a)\\
M_n &= H_n^{(1)'}(\beta_2 b)H_n^{(2)}(\beta_2 c) - H_n^{(1)}(\beta_2 c)H_n^{(2)'}(\beta_2 b)\\
N_n &= H_n^{(1)'}(\beta_2 c)H_n^{(2)'}(\beta_2 b) - H_n^{(1)'}(\beta_2 b)H_n^{(2)'}(\beta_2 c)\\
P_n &= H_n^{(1)'}(\beta_1 b)H_n^{(2)'}(\beta_1 a) - H_n^{(1)'}(\beta_1 a)H_n^{(2)'}(\beta_1 b)\\
Q_n &= H_n^{(1)}(\beta_2 b)H_n^{(2)}(\beta_2 c) - H_n^{(1)}(\beta_2 c)H_n^{(2)}(\beta_2 b)\\
R_n &= H_n^{(1)'}(\beta_2 c)H_n^{(2)}(\beta_2 b) - H_n^{(1)}(\beta_2 b)H_n^{(2)'}(\beta_2 c)
\end{aligned}\right\} \qquad (24)$$

Similarly, after expanding the determinant D', the following is obtained:

$$D' = P\,\beta_1\beta_2\epsilon_2\epsilon_3\left[H_n^{(1)}(\beta_1 b)H_n^{(2)'}(\beta_2 b) - H_n^{(1)'}(\beta_1 b)H_n^{(2)}(\beta_1 b)\right]\times$$
$$\left[H_n^{(1)}(\beta_2 c)H_n^{(2)'}(\beta_2 c) - H_n^{(1)'}(\beta_1 c)H_n^{(2)}(\beta_2 c)\right] \qquad (25)$$

By using the property of the Wronskian determinant equation

$$H_n^{(1)}(z)H_n^{(2)'}(z) - H_n^{(1)'}(z)H_n^{(2)}(z) = -\frac{4i}{\pi z} \quad \text{for all n and } z \neq 0 \qquad (26)$$

it can be shown that Equation 25 can be simplified as follows,

$$D' = -\frac{16\omega\epsilon_1\epsilon_2\epsilon_3}{i\beta_1\pi^2 bc}\frac{E_o}{n\pi}\sin\left(\frac{n\phi_o}{2}\right) \qquad (27)$$

The unknown coefficient D_n is completely determined by Equations 22 through 27. The other coefficients can be determined similarly, and the problem will then be completely solved. The electric field in the far zone (region III) produced by the slotted cylinder is given by

$$E_\phi^{III} = \frac{i\beta_3}{\omega\epsilon_3}\sum_{n=-\infty}^{\infty} D_n H_n^{(2)'}(\beta_3\rho)e^{in\phi}$$
$$\approx \frac{\beta_3}{\omega\epsilon_3}\left(\frac{2}{\pi\beta_3\rho}\right)^{1/2} e^{-i\left(\beta_3\rho-\frac{\pi}{4}\right)}\sum_{n=-\infty}^{\infty} D_n e^{in\left(\phi+\frac{\pi}{2}\right)} \qquad (28)$$

where the coefficient D_n is given by Equation 22. In Equation 28 we have used the asymptotic value of the Hankel function $H_n^{(2)'}(\beta_3\rho)$ for large values of the argument $\beta_3\rho$. From here on we shall use β_o, ϵ_o, η_o instead of β_3, ϵ_3, η_3 to represent the quantities relevant to the region III.

Equation 28 is so complicated that little practical information can be derived from it. In later sections we make various approximations to simplify this expression and thus make it possible to discuss the field in more detail.

2.2. EQUIVALENT PERMITTIVITY OF THE PLASMA SHEATH

It is well known [7, pp. 21-27] that in the absence of a steady magnetic field excitation a quasi-neutral homogeneous plasma can be represented by a homogeneous dielectric medium having a complex permittivity given by

$$\epsilon_2 = \epsilon_o (\epsilon_r - i\sigma_r) \tag{29}$$

where

$$\epsilon_r = 1 - \frac{\omega_p^2}{\omega^2 + \nu^2} \tag{30}$$

$$\sigma_r = \frac{\omega_p^2}{\omega} \frac{\nu}{\omega^2 + \nu^2} \tag{31}$$

ϵ_o is the permittivity of free space

ν is the effective collision frequency

In many practical situations $\omega^2 >> \nu^2$, in which case Equations 30 and 31 can be approximated as follows:

$$\epsilon_r \approx 1 - \frac{\omega_p^2}{\omega^2} \tag{32}$$

$$\sigma_r \approx \frac{\omega_p^2}{\omega^2} \frac{\nu}{\omega} \tag{33}$$

Under this condition, $\sigma_r << \epsilon_r$; consequently the propagation constant β_2 and the intrinsic impedance η_2 of the plasma sheath can be approximated as follows:

$$\beta_2 \approx \beta_o \sqrt{\epsilon_r} \left(1 - i \frac{\sigma_r}{2\epsilon_r}\right) \tag{34}$$

$$\eta_2 \approx \frac{\eta_o}{\sqrt{\epsilon_r}} \left(1 + i \frac{\sigma_r}{2\epsilon_r}\right) \tag{35}$$

where β_o, η_o pertain to free space, and permeability of the plasma has been assumed to be the same as that of free space.

In some other situations where $\omega^2 << \nu^2$, the following approximations are valid:

$$\epsilon_r \approx 1 - \frac{\omega_p^2}{\nu^2} \tag{36}$$

$$\sigma_r \approx \frac{\omega_p^2}{\omega\nu} \tag{37}$$

In Section 6 we consider a special low-frequency case where ω_p, $\nu >> \omega$. In this case the various physical parameters of the plasma can be approximated as follows:

$$\left.\begin{aligned} \epsilon_2 &= \epsilon_o \left(\frac{\omega_p^2}{\omega\nu}\right) e^{-i\pi/2} \\ \beta_2 &= \frac{\beta_o \omega_p}{\sqrt{2\omega\nu}} (1 - i) \\ \eta_2 &= \frac{\eta_o}{\sqrt{2}} \frac{\sqrt{\omega\nu}}{\omega_p} (1 + i) \end{aligned}\right\} \tag{38}$$

3
THIN DIELECTRIC COATING AND PLASMA SHEATH

In this section we determine approximate expressions for the field when both the dielectric coating and the plasma sheath are thin compared to the operating wavelength. We start from the following two assumptions:

$$\begin{aligned} &\beta_1 a, \beta_1 b >> \beta_1 (b - a) \\ &\beta_2 b, \beta_2 c >> \beta_2 (c - b) \end{aligned} \tag{39}$$

where the quantities a, b, c are explained in Figure 2. With the above assumptions, Equations 24 can be approximated by simpler forms. Let us consider the expression for L_n. Using Taylor's expansions for $H_n^{(1),(2)}(\beta, a)$ and $H_n^{(1)',(2)'}(\beta, a)$ in the expression for L_n, we obtain

$$H_n^{(1),(2)}(\beta, a) = H_n^{(1),(2)}(\beta_1 b) + \beta_1(a - b)H_n^{(1)',(2)'}(\beta_1 b) + \ldots$$
$$H_n^{(1)'(2)'}(\beta_1 a) = H_n^{(1)',(2)'}(\beta_1 b) + \beta_1(a - b)H_n^{(1)'',(2)''}(\beta_1 b) + \ldots \quad (40)$$

where '' means differentiating the Hankel functions twice with respect to their total arguments. Substituting Equation 40 in the expression for L_n and retaining the terms of first order in $\beta_1(a - b)$, we obtain

$$L_n \approx \left[H_n^{(1)'}(\beta_1 b)H_n^{(2)}(\beta_1 b) - H_n^{(1)}(\beta_1 b)H_n^{(2)'}(\beta_1 b)\right]$$
$$+ \beta_1(b - a)\left[H_n^{(1)''}(\beta_1 b)H_n^{(2)}(\beta_1 b) - H_n^{(1)}(\beta_1 b)H_n^{(2)''}(\beta_1 b)\right] \quad (41)$$

We now apply the Wronskian determinant equation (26) to Equation 41 and obtain the following for L_n:

$$L_n = \frac{4i}{\pi\beta_1 b}\frac{2b - a}{b} \quad (42)$$

Proceeding similarly, we obtain the following expressions for the other quantities in Equation 24:

$$M_n = \frac{4i}{\pi\beta_2 c}\frac{2c - b}{c} \quad (43)$$

$$N_n = \frac{4i}{\pi}\frac{c - b}{c}\left(1 - \frac{n^2}{\beta_2^2 c^2}\right) \quad (44)$$

$$P_n = \frac{4i}{\pi}\frac{b - a}{b}\left(1 - \frac{n^2}{\beta_1^2 b^2}\right) \quad (45)$$

$$Q_n = \frac{4i}{\pi}\frac{b - c}{c} \quad (46)$$

$$R_n = \frac{4i}{\pi\beta_2 c} \quad (47)$$

Substituting Equations 42 through 47 in Equation 22 gives

$$D_n = (-i)\frac{\frac{E_o}{n\pi}\sin\frac{n\phi_o}{2}}{F_n + G_n} \quad (48)$$

where F_n, G_n are defined as follows:

$$F_n = \frac{2b - a}{b}\left[\eta_o \frac{2c - b}{c} H_n^{(2)'}(\beta_o c) + \eta_2\beta_2(c - b)\left(1 - \frac{n^2}{\beta_2^2 c^2}\right)H_n^{(2)}(\beta_o c)\right] \tag{49}$$

$$G_n = \beta_1(b - a)\left(1 - \frac{n^2}{\beta_1^2 b^2}\right)\left[\beta_o(b - c)\frac{\epsilon_2}{\epsilon_o}\eta_1 H_n^{(2)'}(\beta_o c) + \eta_1 H_n^{(2)}(\beta_o c)\right] \tag{50}$$

As mentioned earlier (Equation 28), the expression for the far zone electric field contains the coefficient given by Equation 38. Expression 28, as it stands, is an infinite series. However, using only the first few coefficients in Equation 48 will usually give accurate enough results. Thus, by using less than some fixed number, say N, it is possible to simplify the numerator in Equation 48; if ϕ_o is sufficiently small,

$$\frac{1}{n}\sin\left(\frac{n\phi_o}{2}\right) \approx \frac{\phi_o}{2}, \quad \text{for} \quad |n| < N \tag{51}$$

Recalling that

$$\left.\begin{aligned} H_{-n}^{(2)}(z) &= (-1)^n H_n^{(2)}(z) \\ H_{-n}^{(2)'}(z) &= (-1)^n H_n^{(2)'}(z) \end{aligned}\right\} \tag{52}$$

we can write Equation 28 as follows:

$$E_\phi \approx \frac{M}{\eta_o} e^{-i\left(\beta_o\rho - \frac{\pi}{4}\right)} P(\phi) \tag{53}$$

where

$$M = \frac{\beta_o}{\omega\epsilon_o}\left(\frac{2}{\pi\beta_o\rho}\right)^{1/2}\frac{(-i)E_o\phi_o}{2\pi} \tag{54}$$

$$P(\phi) = \sum_{n=0}^{N} \frac{\delta_n (i)^n \cos n\phi}{\frac{1}{\eta_o}(F_n + G_n)} \tag{55}$$

$$\begin{aligned} \delta_n &= 1 \quad \text{for } n = 0 \\ &= 2 \quad \text{for } n \neq 0 \end{aligned} \tag{56}$$

In the above, $P(\phi)$ is the radiation pattern of the antenna and is expressed in complex form. The actual radiation pattern is given by the absolute value of $P(\phi)$. Equation 55 is a general expression for the radiation pattern, taking into account the effects of both the dielectric coating and the plasma sheath subject to the assumptions in Equation 39. If we assume that there is no dielectric layer insulating the antenna from the plasma sheath, then a = b, and from Equation 50 we obtain $G_n = 0$. In this case the radiation pattern simplifies to the following:

$$P(\phi) = \sum_{n=0}^{N} \frac{\delta_n (i)^n \cos n\phi}{\frac{2c - b}{c} H_n^{(2)'}(\beta_o c) + \beta_o (c - b)\left(1 - \frac{n^2}{\beta_2^2 c^2}\right) H_n^{(2)}(\beta_o c)} \tag{57}$$

4
THIN DIELECTRIC COATING ONLY

Here it is assumed that only the dielectric coating is thin; i.e., $\beta_1(b - a) << \beta_1 a, \beta_1 b$. It is also assumed that $\beta_2 b, \beta_2 c >> 1$; otherwise we impose no restriction on the thickness of the plasma sheath, i.e., on the quantity $\beta_2(c - b)$. We now make the same approximations as before for the Hankel functions having arguments $\beta_1 a, \beta_1 b$ in Equations 24; for the Hankel functions having arguments $\beta_2 b, \beta_2 c$ we use the usual asymptotic values for large arguments. After making this approximation, we obtain the following:

$$L_n = \frac{4i}{\pi \beta_1 b} \frac{2b - a}{b} \tag{58}$$

$$M_n = \frac{4i}{\pi \beta_2 \sqrt{bc}} \cos \beta_2 (c - b) \tag{59}$$

$$N_n = \frac{4i}{\pi \beta_2 \sqrt{bc}} \sin \beta_2 (c - b) \tag{60}$$

$$P_n = \frac{4i}{\pi} \frac{b - a}{b} \left(1 - \frac{n^2}{\beta_1^2 b^2}\right) \tag{61}$$

$$Q_n = - \frac{4i}{\pi \beta_2 \sqrt{bc}} \sin \beta_2 (c - b) \tag{62}$$

$$R_n = \frac{4i}{\pi \beta_2 \sqrt{bc}} \cos \beta_2 (c - b) \tag{63}$$

Using Equations 22, and 58 through 63, we obtain the following after some algebraic manipulation:

$$D_n = (-i)\frac{\frac{E_o}{n\pi}\sin\left(\frac{n\phi_o}{2}\right)\left(\frac{b}{c}\right)^{1/2}}{A_n + B_n} \tag{64}$$

where

$$A_n = \frac{2b - a}{b}\left[\eta_o H_n^{(2)'}(\beta_o c)\cos\beta_2(c - b) + \eta_2 H_n^{(2)}(\beta_o c)\sin\beta_2(c - b)\right] \tag{65}$$

$$B_n = \beta_2(b - a)\left(1 - \frac{n^2}{\beta_1^2 b^2}\right)\left[\eta_2 H_n^{(2)}(\beta_o c)\cos\beta_2(c - b) - \eta_o H_n^{(2)'}(\beta_o c)\sin\beta_2(c - b)\right] \tag{66}$$

It can now be shown that the far zone electric field in this case is given by an equation similar to Equation 53, and the pattern factor is given by the following:

$$P(\phi) = \sum_{n=0}^{N} \frac{\delta_n (i)^n \cos n\phi}{\frac{1}{\eta_o}(A_n + B_n)} \tag{67}$$

After introducing the explicit expressions for β_2, η_2 for the plasma sheath in Equations 65 and 66, we can rewrite Equation 67 as follows:

$$P(\phi) = \sum_{n=0}^{N} \frac{\delta_n (i)^n \cos n\phi}{A'_n + B'_n} \tag{68}$$

where

$$A'_n = \frac{2b - a}{b}\left\{\left[F_1 H_n^{(2)'}(x_o) + \frac{1}{\sqrt{\epsilon_r}} H_n^{(2)}(x_o)\left(F_3 + \frac{\sigma_r}{2\epsilon_r} F_4\right)\right]\right.$$
$$\left. + i\left[F_2 H_n^{(2)'}(x_o) - \frac{1}{\sqrt{\epsilon_r}} H_n^{(2)}(x_o)\left(F_4 - \frac{\sigma_r}{2\epsilon_r} F_3\right)\right]\right\} \tag{69}$$

$$B'_n = \beta_o(b - a)\left(1 - \frac{n^2}{\beta_1^2 b^2}\right)\left\{\left[F_1 H_n^{(2)}(x_o) - \sqrt{\epsilon_r} H_n^{(2)'}(x_o)\left(F_3 - \frac{\sigma_r}{2\epsilon_r} F_4\right)\right]\right.$$
$$\left. + i\left[F_2 H_n^{(2)}(x_o) + \sqrt{\epsilon_r} H_n^{(2)'}(x_o)\left(F_4 + \frac{\sigma_r}{2\epsilon_r} F_3\right)\right]\right\} \tag{70}$$

$$\left.\begin{aligned} F_1 &= \cos x_1 \cosh x_2 \\ F_2 &= \sin x_1 \sinh x_2 \\ F_3 &= \sin x_1 \cosh x_2 \\ F_4 &= \cos x_1 \sinh x_2 \end{aligned}\right\} \tag{71}$$

$$x_1 = \beta_o \sqrt{\epsilon_r}\,(c - b) \tag{72}$$

$$x_2 = \frac{\beta_o \sigma_r}{2\sqrt{\epsilon_r}}(c - b) \tag{73}$$

$$\beta_2 = x_1 - ix_2 \tag{74}$$

$$x_o = \beta_o c \tag{75}$$

Let us now assume that $x_2 << 1$; physically this means that the collision frequency ν is very small. Under this condition we can write $F_1 \approx \cos x_1$, $F_3 \approx \sin x_1$, and $F_2 \approx F_4 \approx 0$, and obtain the following:

$$A'_n = \frac{2b - a}{b}\left\{\left[\cos x_1 H_n^{(2)'}(x_o) + \frac{1 + \frac{i\sigma_r}{2\epsilon_r}}{\sqrt{\epsilon_r}} \sin x_1 H_n^{(2)}(x_o)\right]\right\} \tag{76}$$

$$B'_n = \beta_o(b - a)\left(1 - \frac{n^2}{\beta_1^2 b^2}\right)\left[\cos x_1 H_n^{(2)}(x_o) - \sqrt{\epsilon_r}\left(1 - \frac{i\sigma_r}{2\epsilon_r}\right) \sin x_1 H_n^{(2)'}(x_o)\right] \tag{77}$$

The collisionless case is obtained from the above by making the substitution $\sigma_r = 0$. As before, if the effect of the dielectric coating is negligible (b = a), we get $B'_n = 0$.

5
APPROXIMATION FOR HIGH FREQUENCY

In this section we discuss the radiation pattern, as derived above, which arises when the operating frequency is higher than the plasma frequency. A collisionless plasma is transparent to the electromagnetic waves when $\omega > \omega_p$; but the discontinuity in the permittivity will cause reflection. When the collision effects are important, the plasma bahaves like a lossy dielectric, and consequently the wave will also be attenuated.

For this range of frequency it is reasonable to assume that $\omega >> \nu$. As mentioned before (Equations 32 through 34), under these circumstances the physical parameters of the plasma sheath can be written in the following form:

$$\left.\begin{aligned} \epsilon_r &\approx 1 - \frac{\omega_p^2}{\omega^2} \\ \sigma_r &\approx \frac{\omega_p^2}{\omega^2}(\nu/\omega) \\ \beta_2 &\approx \beta_o \sqrt{\epsilon_r}\left(1 - i\frac{\sigma_r}{2\epsilon_r}\right) \\ \eta_2 &\approx \frac{\eta_o}{\sqrt{\epsilon_r}}\left(1 + i\frac{\sigma_r}{2\epsilon_r}\right) \end{aligned}\right\} \tag{78}$$

After substituting Equation 78 in Equation 55, we obtain the following for the radiation pattern when both the dielectric coating and the plasma sheath are thin:

$$P(\phi) = \sum_{n=0}^{N} \frac{\delta_n (i)^n \cos n\phi}{F'_n + G'_n} \tag{79}$$

where

$$F'_n = \frac{2b - a}{b}\left\{\frac{2c - b}{c} H_n^{(2)'}(x_o) + \beta_o(c - b)\left[1 - \frac{n^2}{\beta_o^2 \epsilon_r c^2}\left(1 + i\frac{\sigma_r}{\epsilon_r}\right)\right] H_n^{(2)}(x_o)\right\} \tag{80}$$

$$G'_n = \beta_o(b - a)\left(1 - \frac{n^2}{\beta_1^2 b^2}\right)\left[\beta_o(b - c)\epsilon_r\left(1 - i\frac{\sigma_r}{\epsilon_r}\right) H_n^{(2)'}(x_o) + H_n^{(2)}(x_o)\right] \tag{81}$$

where $x_o = \beta_o c$. In the absence of the dielectric coating, b = a and Equation 79 can be simplified to the following form:

$$P(\phi) = \sum_{n=0}^{N} \frac{\delta_n (i)^n \cos n\phi}{\frac{2c - b}{c} H_n^{(2)'}(x_o) + \beta_o(c - b)\left[1 - \frac{n^2 \omega_p^2}{\beta_o^2\left(1 - \frac{\omega_p^2}{\omega^2}\right)c^2}\left(1 + i\frac{\sigma_r}{\epsilon_r}\right)\right] H_n^{(2)}(x_o)} \tag{82}$$

In the absence of collision the corresponding radiation patterns can be obtained from Equations 79 and 82 by substituting $\sigma_r = 0$.

The radiation pattern for a thick plasma sheath is discussed in Section 4. In the absence of the dielectric coating and for $\omega > \omega_p$, the radiation pattern is obtained from Equation 68 as follows ($B'_n = 0$):

$$P(\phi) = \sum_{n=0}^{N} \frac{\delta_n (i)^n \cos n\phi}{H_n^{(2)'}(x_o) \cos x_1 + \frac{\left(1 + i\frac{\sigma_r}{2\epsilon_r}\right)}{\left(1 - \frac{\omega_p^2}{\omega^2}\right)^{1/2}} \sin x_1 H_n^{(2)}(x_o)} \tag{83}$$

where

$$x_1 = \beta_o \left(1 - \frac{\omega_p^2}{\omega^2}\right)^{1/2} (c - b) \tag{84}$$

As a check on our pattern expression, we note that in the absence of both the dielectric coating and the plasma sheath ($a = b = c$, $\epsilon_1 = \epsilon_2 = \epsilon_o$), Equations 82 and 83 reduce to the familiar form:

$$P(\phi) = \sum_{n=0}^{N} \frac{\delta_n (i)^n \cos n\phi}{H_n^{(2)'}(x_o)} \tag{85}$$

6
APPROXIMATION FOR LOW FREQUENCY

When the operating frequency is lower than the plasma frequency, the plasma is opaque to the electromagnetic wave [8] —the wave passing through the sheath suffers attenuation whether collision effects are important or not. In the following we consider separately the two cases when the collision effect is negligible and when it is important. In both the cases it is assumed that $\omega << \omega_p$.

Case (i): In a collisionless plasma we can use the following approximations:

$$\begin{aligned} \epsilon_r &\approx -\frac{\omega_p^2}{\omega^2} \\ \sigma_r &= 0 \\ \beta_2 &\approx i\,\beta_0\left(\frac{\omega_p}{\omega}\right) \\ \tau_2 &\approx -i\,\eta_0\left(\frac{\omega}{\omega_p}\right) \end{aligned} \tag{86}$$

We first consider the case when both the dielectric crating and the plasma sheath are thin. Substituting Equation 86 in Equation 55 gives the following for the pattern:

$$P(\phi) = \sum_{n=0}^{N} \frac{\delta_n (i)^n \cos n\phi}{F'_n + G'_n} \tag{86a}$$

where

$$F'_n = \frac{2b - a}{b}\left[\frac{2c - b}{c} H_n^{(2)'}(x_o) + \beta_o(c - b)\left(1 + \frac{n^2\omega^2}{\beta_o^2\omega_p^2c^2}\right) H_n^{(2)}(x_o)\right] \tag{86b}$$

$$G'_n = \beta_o(b - a)\left(1 - \frac{n^2}{\beta_1^2b^2}\right)\left[H_n^{(2)}(x_o) - \beta_o(b - c)\frac{\omega_p^2}{\omega^2} H_n^{(2)'}(x_o)\right] \tag{87}$$

In the absence of the dielectric coating $G'_n = 0$ in the above equation.

If the dielectric coating only is thin, the pattern is given by Equation 86a, and F'_n and G'_n are given by the following:

$$F'_n = \frac{2b - a}{b}\left[H_n^{(2)'}(x_o)\cosh\frac{\beta_o\omega_p}{\omega}(c - b) + \frac{\omega}{\omega_p} H_n^{(2)}(x_o)\sinh\frac{\beta_o\omega_p}{\omega}(c - b)\right] \tag{88}$$

$$G'_n = \beta_o(b - a)\left(1 - \frac{n^2}{\beta_1^2b^2}\right)\left[H_n^{(2)}(x_o)\cosh\frac{\beta_o\omega_p}{\omega}(c - b) - \frac{\omega_p}{\omega} H_n^{(2)'}(x_o)\sinh\frac{\beta_o\omega_p}{\omega}(c - b)\right] \tag{89}$$

In the absence of the dielectric coating $G'_n = 0$ and if $\frac{\beta_o \omega_p}{\omega}(c - b) >> 1$, then the pattern is given by the following:

$$P(\phi) = \sum_{n=o}^{N} \frac{2\,\delta_n (i)^n \cos n\phi\, e^{-\frac{\beta_o \omega_p}{\omega}(c-b)}}{H_n^{(2)'}(x_o) + \frac{\omega}{\omega_p} H_n^{(2)}(x_o)} \tag{90}$$

As expected, Equation 90 shows that the fields are attenuated exponentially in passing through the sheath; the attenuation in nepers can be expressed as follows:

$$\alpha_{\text{nepers}} = \frac{\beta_o \omega_p}{\omega}(c - b) \tag{91}$$

Case (ii): Here we consider the above two cases, taking into account the effect of collision. As mentioned in Section 2, if $\omega_p, \nu >> \omega$, the plasma sheath parameters can be approximated as follows:

$$\epsilon_2 = \epsilon_o \left(\frac{\omega_p^2}{\omega\nu}\right) e^{-i\pi/2}$$

$$\beta_2 = \frac{\beta_o \omega_p}{\sqrt{2\omega\nu}}(1 - i) \tag{92}$$

$$\eta_2 = \frac{\eta_o}{\sqrt{2}} \frac{\sqrt{\omega\nu}}{\omega_p}(1 + i)$$

The radiation pattern in this case is obtained from Equation 62, A'_n and B'_n being given by the following:

$$A'_n = \frac{2b - a}{b}\left\{P\, H_n^{(2)'}(x_o) + \frac{\sqrt{2\omega\nu}}{\omega_p}(R + S) H_n^{(2)}(x_o) + i\left[Q\, H_n^{(2)'}(x_o) + \frac{\sqrt{2\omega\nu}}{\omega_p}(R - S) H_n^{(2)}(x_o)\right]\right\} \tag{93}$$

$$B'_n = \eta_o (b - a)\left(1 - \frac{n^2}{\beta_1^2 b^2}\right)\left\{P\, H_n^{(2)}(x_o) - \frac{\omega_p}{\sqrt{2\omega\nu}}(R - S) H_n^{(2)'}(x_o) + i\left[Q\, H_n^{(2)'}(x_o) + \frac{\omega_p}{\sqrt{2\omega\nu}}(R + S) H_n^{(2)}(x_o)\right]\right\} \tag{94}$$

where

$$\left.\begin{aligned} P &= \cos x_3 \cosh x_3 \\ Q &= \sin x_3 \sinh x_3 \\ R &= \sin x_3 \cosh x_3 \\ S &= \cos x_3 \sinh x_3 \end{aligned}\right\} \tag{95}$$

$$x_3 = \frac{\beta_o \omega_p}{\sqrt{2\omega\nu}} (c - b) \tag{96}$$

If the slotted cylinder is in direct contact with the plasma sheath, then b = a, and we obtain the following for the pattern:

$$P(\phi) = \sum_{n=o}^{N} \frac{\delta_n (i)^n \cos n\phi}{P H_n^{(2)'}(x_o) + \frac{\sqrt{2\omega\nu}}{\omega_p}(R + S) H_n^{(2)}(x_o) + i\left[Q H_n^{(2)'}(x_o) + \frac{\sqrt{2\omega\nu}}{\omega_p}(R - S) H_n^{(2)}(x_o)\right]} \tag{97}$$

Equation 97 can be further simplified for the following two special cases.

(a) Let $x_3 >> 1$; i.e., $\beta_o(c - b) >> \sqrt{2\omega\nu}/\omega_p$. This assumption means that the plasma sheath is thick. Here we can use the approximation $\cosh x_3 \approx \sinh x_3 \approx e^{x_3}/2$ in Equation 95, and we obtain the following from Equation 97:

$$P(\phi) = \sum_{n=o}^{N} \frac{2\,\delta_n (i)^n \cos n\phi\, e^{-ix_3} e^{-x_3}}{H_n^{(2)'}(x_o) + \frac{\sqrt{2\omega\nu}}{\omega_p} H_n^{(2)}(x_o)(1 - i)} \tag{98}$$

The attenuation of the wave in passing through the sheath can be expressed approximately as follows:

$$\alpha_{\text{nepers}} = \frac{\beta_o \omega_p}{\sqrt{2\omega\nu}} (c - b) \tag{99}$$

Interestingly enough, Equation 99 predicts that in a physical situation where the underlying assumptions are true, the collision effects help in reducing the attenuation of the electromagnetic waves moving through the plasma sheath.

(b) Let $x_3 << 1$; i.e., $\beta_o(c - b) << \sqrt{2\omega\nu}/\omega_p$; that is, assume that the plasma sheath is very thin. We can then use the following approximations: $\cos x_3 \approx \cosh x_3 \approx x_1$, $\sin x_3 \approx \sinh x_3 \approx x_3$. Thus we obtain the following from Equation 97:

$$P(\phi) = \sum_{n=0}^{N} \frac{\delta_n (i)^n \cos n\phi}{H_n^{(2)'}(x_o) + 2\beta_o (c - b) H_n^{(2)}(x_o)} \qquad (100)$$

It can be seen from this equation that to a first order of approximation the pattern is independent of ν and ω_p but depends on the thickness of the plasma sheath.

7
NUMERICAL RESULTS

This section gives results obtained from numerical computations of some of the expressions derived in the previous sections. Only results from the approximate formulas have been obtained; results from the exact expressions would require extensive and tedious computations.

All of the field expressions obtained are in the form of infinite series. If the radius of the conducting cylinder is small ($\beta_o a < 1$) compared to the free space wavelength, the series converges rapidly and a few leading terms in the series are sufficient for obtaining reasonably accurate results. If the radius is large ($\beta_o a > 1$), the series converge slowly, and usually a large number of terms should be included in computing the series for even moderately accurate results. For slots in large cylinders special mathematical methods have been developed [2] for good numerical results. In the present case, however, we do not consider those methods. Since we are primarily interested in the general effects of the plasma sheath on the radiation pattern, it will be sufficient to use the above approximate procedure.

If the angular width ϕ_o of the slot is sufficiently small, then $\frac{\sin n\phi_o}{n\phi_o} \approx 1$ over the range of n for which the terms of the series are significant. This can be seen in Table I (taken from Reference 6), which shows the dependence on x of the number of terms required for five-figure accuracy and the associated value of ϕ_o for which $\frac{\sin n\phi_o}{n\phi_o} \geq 0.9$ over the range of n. It is evident from the table that the necessary number of terms n increases with increase of the argument x of the Hankel functions. In the present problem we have computed the radiation patterns by using the first fifteen terms of the infinite series.[1] The particular values of the various physical parameters are assumed for convenience of computation, and may not apply directly to a real case. Nevertheless the results bring out clearly the influence of the different plasma param-

[1]The Hankel functions for the arguments used here are not readily available in standard tables. For this reason the computed values of the Bessel and Neumann functions for the arguments used here are shown in the appendix.

TABLE I. VALUES FOR WHICH $\frac{H_o^{(2)'}(x)}{H_n^{(2)'}(x)} < 0.0001$ AND $\frac{\sin n\phi_o}{n\phi_o} > 0.9$

x:	0.5	1.0	1.5	2.0	3	3.5	4	5
n:	5	6	8	9	10	13	13	13
ϕ_o(rad):	0.158	0.132	0.088	0.079	0.079	0.061	0.061	0.061

eters on the radiation produced by the antenna. All the patterns computed here are individually normalized to unity; consequently it is not possible to compare the absolute values of the amplitudes in the different cases.

In order to facilitate the identification of the radiation patterns reported in the following sections, the various physical parameters associated with the different parameters are shown in Table II. In all cases $\omega = 2\pi \times 10^{10}$, $\beta_o a = 5$, $\beta_o b = 5.1$, $\epsilon_1 = 4$.

TABLE II. PHYSICAL PARAMETERS ASSOCIATED WITH DIFFERENT FIGURES

Fig. No.	ω_p	ν	$\beta_o c$
3	0	0	5.1
4	$\omega/4$	10^8	5.3
5(a)	$\omega/2$	10^8	5.3
5(b)	$\omega/1.5$	10^8	5.3
5(c)	$\omega/1.1$	10^8	5.3
6(a)	$\omega/4$	12ω	5.3
6(b)	$\omega/4$	20ω	5.3
7(a)	$\omega/4$	10^8	5.5
7(b)	$\omega/4$	10^8	8.1
8	$\omega/4$	10^8	8.6
9	2ω	0	5.3
10	5ω	0	5.4
11	10ω	0	5.4

In Figure 3 is shown the radiation pattern produced by the dielectric coated slotted cylinder antenna in the absence of plasma sheath. It has been computed by using Equations 48 through 50, after making the assumptions b = c, $\epsilon_2 = \epsilon_0$. The calculated pattern compares favorably with known results [2]. In the following sections, where the influence of the plasma sheath on the radiation characteristics of the antenna is discussed, the pattern given by Figure 3 will be taken as the standard for comparison; henceforth it will be referred to as the free space pattern.

Figure 4 shows the radiation pattern produced by the antenna in the presence of a thin plasma sheath when the operating frequency is higher than the plasma frequency. The general shape of this pattern is not appreciably different from the free space pattern, except that the response in the backward direction is increased slightly.

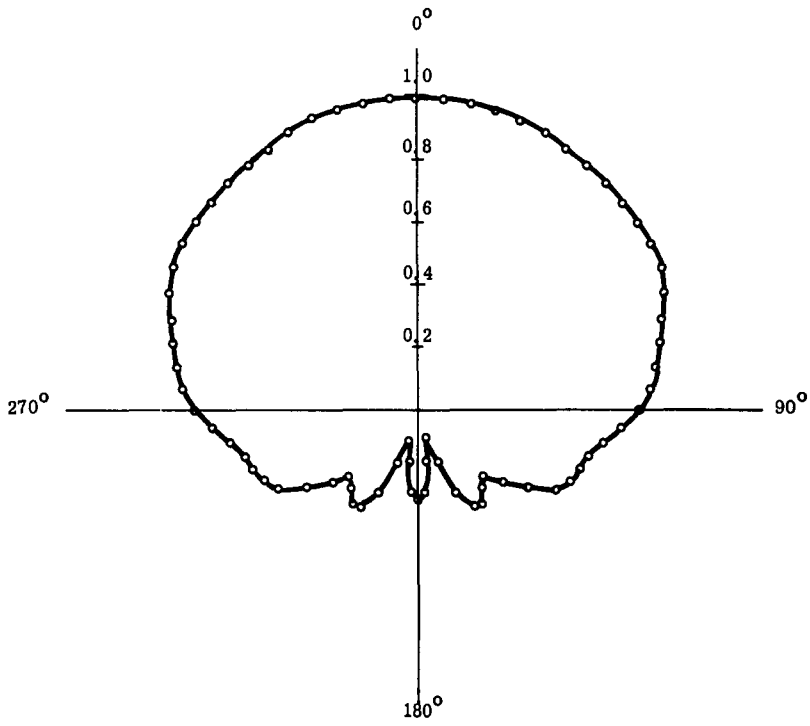

FIGURE 3. THE RADIATION PATTERN OF THE DIELECTRIC-COATED SLOTTED CYLINDER. Thickness of the dielectric layer = β_0 (b - a) = 0.1; $\beta_0 a$ = 5; dielectric constant of the insulating layer = ϵ_1 = 4.

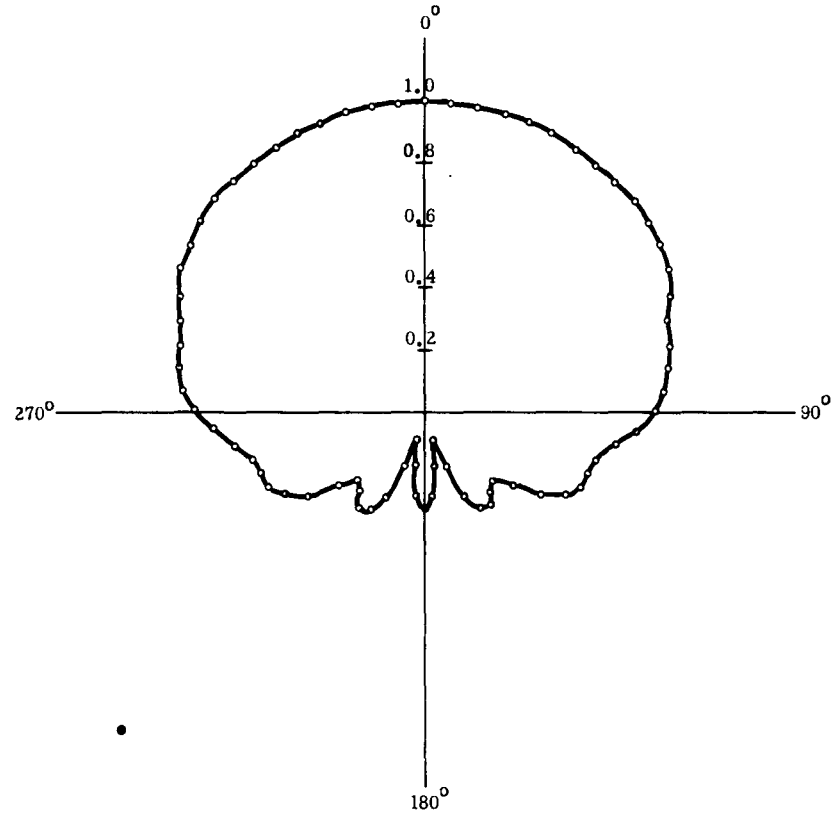

FIGURE 4. RADIATION PATTERN OF THE PLASMA-COVERED SLOTTED CYLINDER. Normalized plasma thickness, β_o (c - b) = 0.2: β_oa = 5: β_ob = 5.1: β_oc = 5.3: $\omega = 2\pi \times 10^{10}$; $\nu = 10^8$; $\omega_p = 2\omega/4$: $\epsilon_1 = 4$.

In Figure 5 are shown the patterns produced by the antenna in the presence of a plasma sheath, for an operating frequency higher than the plasma frequency and for various values of ω_p/ω. These patterns, which refer to the cases in which both the dielectric coating and the plasma sheath are thin, were computed by using Equations 48 through 50. From Figures 3, 4, and 5 it can be seen that for $\omega \geq 2\omega_p$ the pattern does not differ appreciably from the free space pattern. In fact, as expected, the pattern approaches the free space case for $\omega >> \omega_p$. The reason is that when the operating frequency is much higher than the plasma frequency, the equivalent permittivity of the plasma sheath almost equals the free space permittivity. Therefore, the pattern does not change appreciably with the change of ω_p/ω when $\omega >> \omega_p$. As ω_p/ω

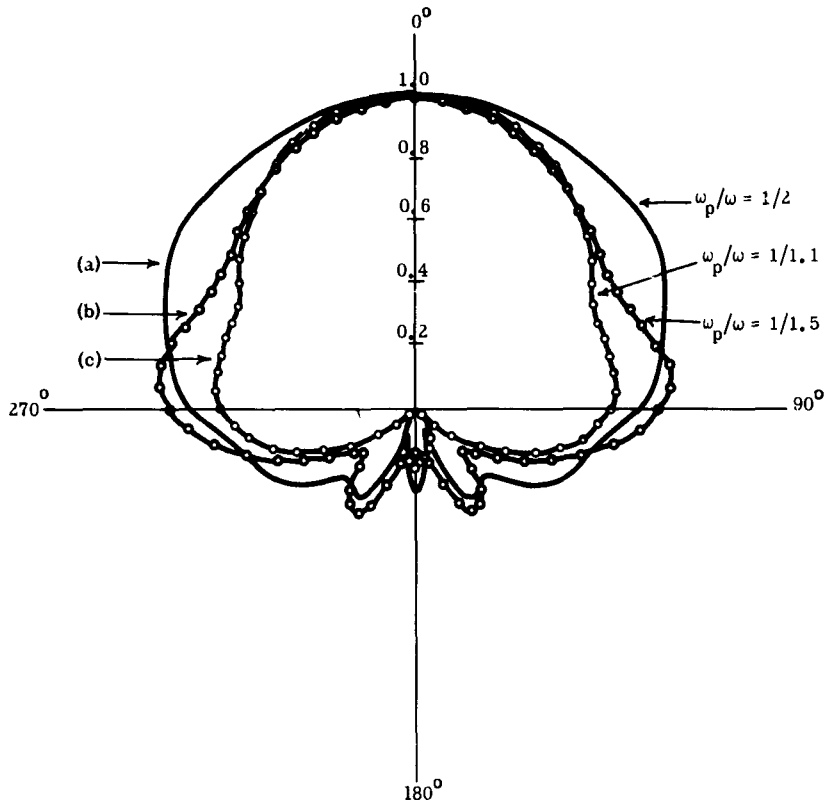

FIGURE 5. RADIATION PATTERN OF THE PLASMA-COVERED SLOTTED CYLINDER WITH ω_p/ω AS A PARAMETER. Normalized plasma thickness = β_o (c - b) = 0.2; β_oa = 5; β_ob = 5.1; β_oc = 5.3; $\omega = 2\pi \times 10^{10}$; $\nu = 10^8$; $\epsilon_1 = 4$.

approaches unity, however, the pattern changes significantly, because when ω_p/ω is close to unity the equivalent permittivity of the plasma sheath differs considerably from the free space permittivity and varies rapidly with ω_p/ω. In general, it may be concluded from Figure 5 that as ω_p/ω approaches unity the pattern becomes more and more directional.

In order to investigate the influence of collision frequency, the radiation pattern of the antenna has been computed, by Equations 48 through 50, for $\omega_p/\omega = 1/4$ and for various values of the collision frequency ν. The other parameters are as explained in Figure 6. Of the many patterns calculated for different values of ν, only two representative ones are shown. It has been found that for collision frequencies up to $\nu = 4\omega$ the radiation pattern does not change ap-

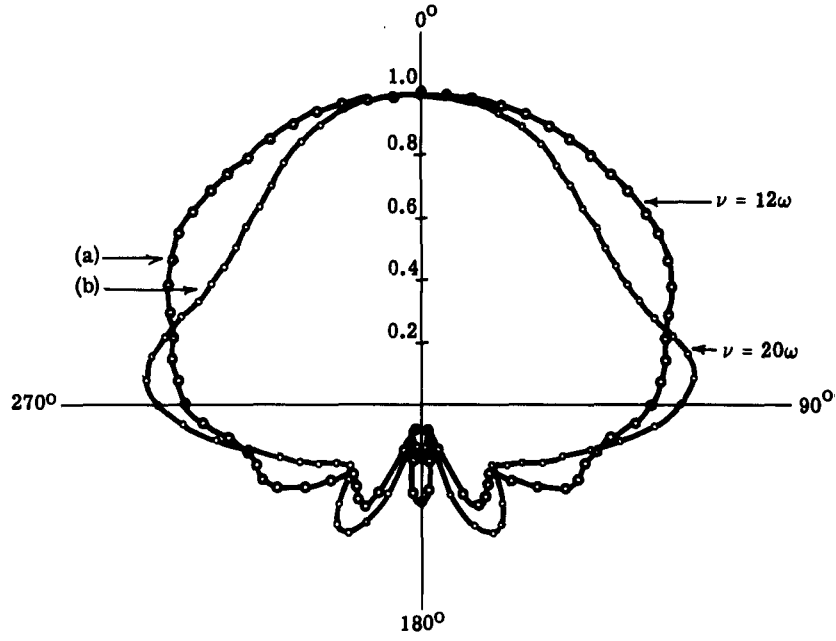

FIGURE 6. RADIATION PATTERN OF THE PLASMA-COVERED SLOTTED CYLINDER WITH COLLISION FREQUENCY AS A PARAMETER. $\beta_0 a = 5$; $\beta_0 b = 5.1$; $\beta_0 c = 5.3$; $\omega = 2\pi \times 10^{10}$; $\omega_p = \omega/4$; $\epsilon_1 = 4$.

preciably with the change of ν except that an increase in ν slightly increases the back radiation from the antenna. It can be seen from Figure 6 that for $\nu = 20\omega$ the pattern is more directional than in the free space case and new side lobes start to appear.

Figures 7 and 8 show the radiation patterns produced by the antenna for $\omega_p/\omega = 1/4$ and for different thicknesses of the plasma sheath. The pattern for $\beta_0(c - b) = 0.4$ has been calculated from Equations 48 through 50. The patterns for $\beta_1(c - b) = 3$ and 3.5 have been computed from Equations 68, 76, and 77. It can be seen from Figure 7 that as the plasma sheath becomes thicker the pattern becomes more directional, and at the same time the pattern becomes smoother than in the free space case. In Figure 8, where $\beta_0(c - b) = 3.5$, the effect of the plasma sheath is very significant: many lobes appear in the radiation pattern. They can be attributed to waves present within the plasma sheath and traveling along the circumference of the cylinder.

In Figures 9, 10, and 11 are plotted the radiation patterns for different values of ω_p/ω, for an operating frequency lower than the plasma frequency. These patterns are obtained from

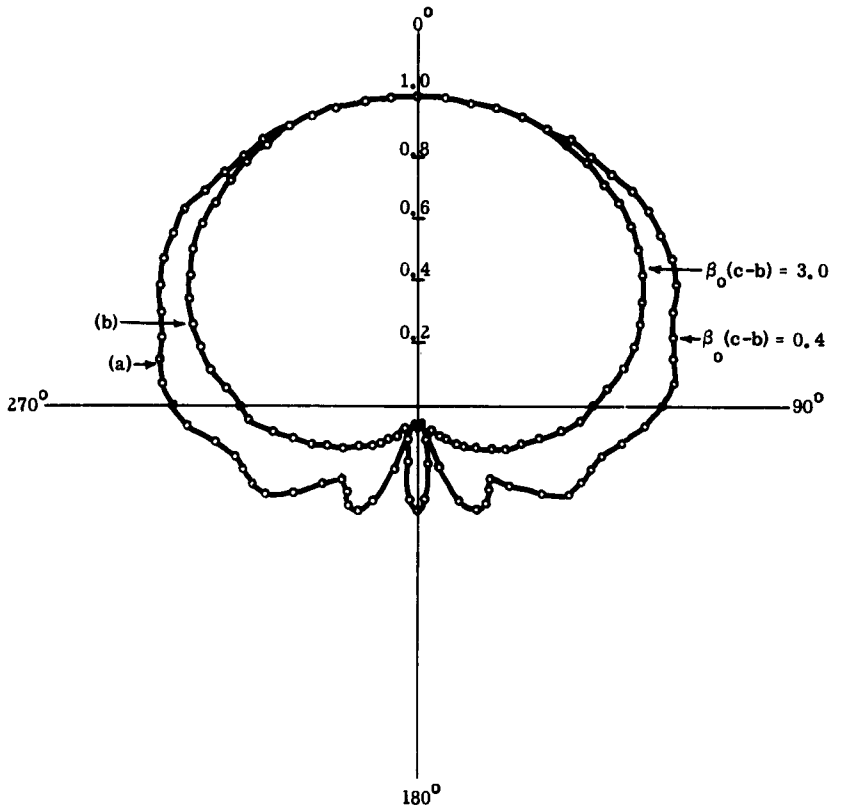

FIGURE 7. RADIATION PATTERN OF THE PLASMA-COVERED SLOTTED CYLINDER WITH PLASMA SHEATH THICKNESS AS A PARAMETER. $\beta_o a = 5$; $\beta_o b = 5.1$; $\omega = 2\pi \times 10^{10}$; $\omega_p = \omega/4$; $\nu = 10^8$; $\epsilon_1 = 4$.

Equations 85 through 87, where the plasma has been assumed to be collision free. For $\omega < \omega_p$ the boundaries of the plasma sheath reflect nearly all the evanscent electromagnetic waves within the plasma sheath. The few waves which are transmitted to free space account for the radiation field, whose absolute value is considerably less than when $\omega < \omega_p$. The many lobes in the patterns may be due to standing waves within the plasma sheath.

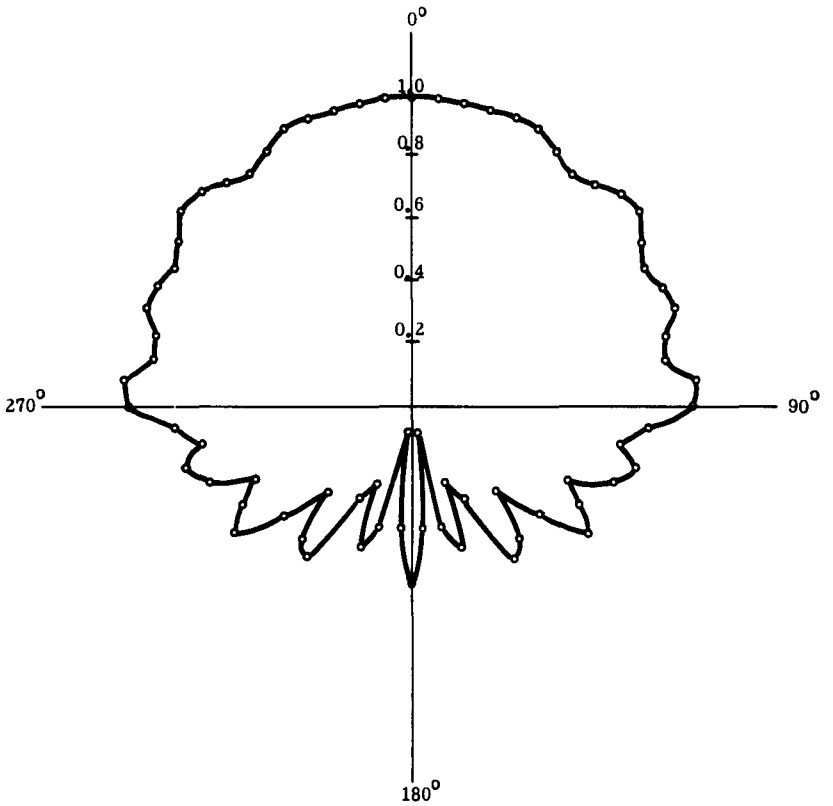

FIGURE 8. RADIATION PATTERN OF THE PLASMA-COVERED SLOTTED CYLINDER FOR NORMALIZED PLASMA THICKNESS. $\beta_0 (c - b) = 3.5$; $\beta_0 a = 5$; $\beta_0 b = 5.1$; $\beta_0 c = 8.6$; $\omega = 2\pi \times 10^{10}$; $\omega_p = \omega/4$; $\nu = 10^8$; $\epsilon_1 = 4$.

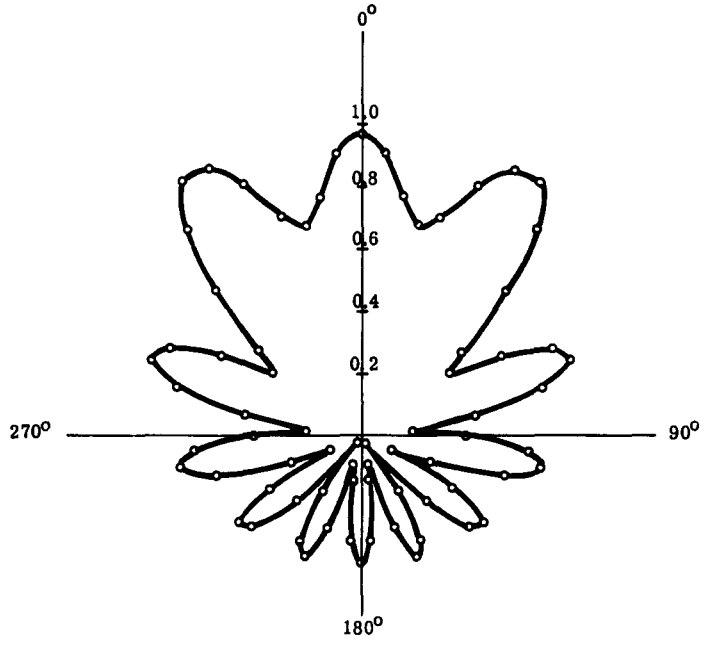

FIGURE 9. RADIATION PATTERN OF THE PLASMA-COVERED SLOTTED CYLINDER FOR THE CASE IN WHICH $\beta_o a = 5$, $\beta_o b = 5.1$, $\beta_o c = 5.3$, $\omega = 2\pi \times 10^{10}$, $\nu = 0$, $\omega_p = 2\omega$, AND $\epsilon_1 = 4$.

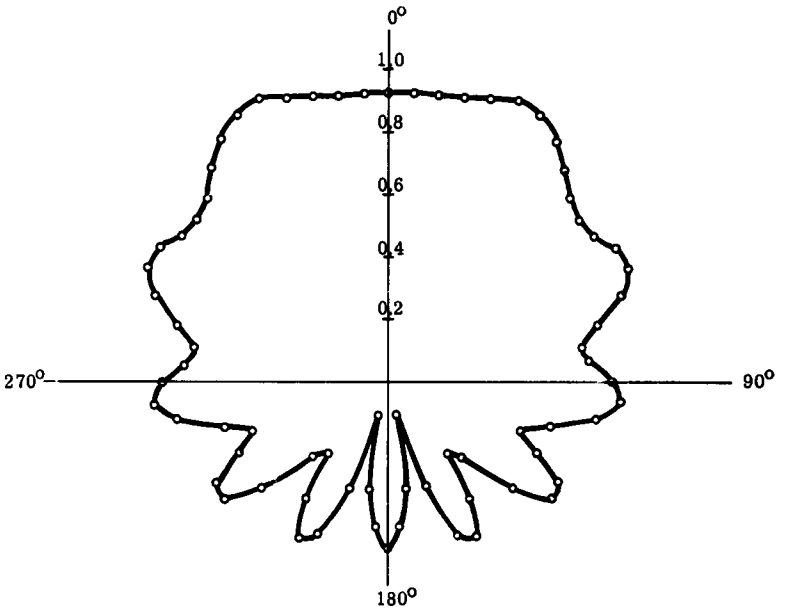

FIGURE 10. RADIATION PATTERN OF THE PLASMA-COVERED SLOTTED CYLINDER FOR THE CASE IN WHICH $\beta_0 a = 5$, $\beta_0 b = 5.1$, $\beta_0 c = 5.3$, $\omega = 2\pi \times 10^{10}$, $\nu = 0$, $\omega_p = 5\omega$, AND $\epsilon_1 = 4$.

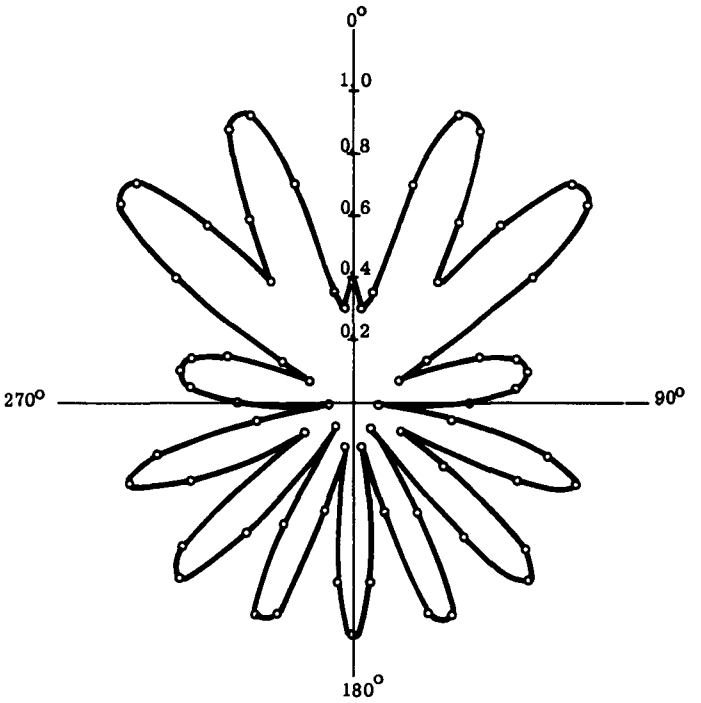

FIGURE 11. RADIATION PATTERN OF THE PLASMA-COVERED SLOTTED CYLINDER FOR THE CASE IN WHICH $\beta_0 a = 5$, $\beta_0 b = 5.1$, $\beta_0 c = 5.3$, $\omega = 2\pi \times 10^{10}$, $\nu = 0$, $\omega_p = 10\omega$, AND $\epsilon_1 = 4$.

8
CONCLUSIONS

We have discussed in detail the far zone electric field produced by an infinite slot in an infinite cylinder surrounded by a homogeneous plasma sheath. We have considered the cases when $\omega > \omega_p$ and $\omega < \omega_p$. Explicit expressions for the azimuthal radiation pattern are given for various physical situations. These expressions can be used to determine the azimuthal radiation pattern of a similarly excited finite axial slot in a conducting cylinder of infinite length surrounded by a plasma sheath. The expressions given apply whether or not there is collision in the plasma. From the numerical results given, the following general conclusions can be made about the effect of plasma sheath on the radiation pattern produced by the infinite slot antenna.

(1) For $\omega < \omega_p$.

A collisionless plasma sheath reduces the amplitude of the field by an amount $e^{-\frac{\beta_o \omega_p}{\omega}(c-b)}$ and introduces many nulls in the radiation pattern. In the special case when $\omega_p, \nu >> \omega$, the increase of collision frequency helps to reduce the attenuation of the field.

(2) For $\omega > \omega_p$.

(a) The radiation pattern narrows more and more and new side lobes appear in the pattern as ω_p/ω approaches unity. For $\omega \geq 2\omega_p$ the pattern does not change appreciably for a change in ω_p/ω.

(b) For collision frequencies $\nu < 4\omega$, the collision effects do not change the shape of the pattern appreciably except that the back radiation from the antenna is enhanced slightly if ν is increased. For $\nu >> 4\omega$ the pattern becomes more directional, and minor lobes appear in the pattern with increase of ν.

(c) As the plasma sheath becomes thicker, at first the pattern becomes smooth and more directional; when it is very thick, minor lobes appear in the pattern.

The physical explanation of how the different plasma parameters influence the pattern, and the detailed reasons for the deterioration of the radiation patterns produced by the antenna in various cases, are not obvious from the results reported in the present study.

Appendix
NUMERICAL COMPUTATION OF BESSEL FUNCTIONS

During the computation procedure, the Hankel functions are expressed as $H_n^{(2)}(x) = J_n(x) - iY_n(x)$, where $J_n(x)$ and $Y_n(x)$ are the standard notations for n-th order Bessel and Neumann functions respectively. The values of $Y_o(x)$ and $Y_1(x)$ are taken from the tables given in Reference 9. The values of $Y_n(x)$ for n = 2 to n = 15 are calculated from the recursion relation $Y_{n+1}(x) = \frac{2n}{x} Y_n(x) - Y_{n-1}(x)$. The values of $J_n(x)$ for n = 0 to n = 15 are taken from the NBS Tables of Bessel Functions. $J'_n(x)$ and $Y'_n(x)$ are computed from the recursion relation $C'_n(x) = \frac{1}{2} C_{n-1}(x) - C_{n+1}(x)$, where C_n stands for J_n or Y_n. The calculated values of the various functions are shown in Tables III through VI.

TABLE III. VALUES FOR $J_n(x)$

n \ x	5.3	5.4	5.5	8.1	8.6
0	-0.075803	-0.041210	-0.006844	0.147517	0.014623
1	-0.345961	-0.345345	-0.341438	0.247608	0.272755
2	-0.054748	-0.086695	-0.117315	-0.086380	0.048808
3	+0.304641	+0.281126	+0.256118	-0.290264	-0.250053
4	+0.399625	+0.399058	+0.396717	-0.128631	-0.223264
5	+0.298567	+0.310070	+0.320925	+0.163222	0.042366
6	+0.163708	+0.175147	+0.186783	+0.330139	0.272527
7	+0.072093	+0.079145	+0.086601	+0.325873	0.337904
8	+0.026725	+0.030044	+0.033657	+0.233099	0.277550
9	+0.008588	+0.009873	+0.011309	+0.134568	0.178467
10	+0.002441	+0.002868	+0.003356	+0.065943	0.095987
11	+0.000623	+0.000747	+0.000893	+0.028253	0.044758
12	+0.000144	+0.000177	+0.000216	+0.010794	0.018510
13	+0.000031	+0.000038	+0.000048	+0.003730	0.006898
14	+0.000006	+0.000008	+0.000010	+0.001178	0.002344
15	+0.000001	+0.000001	+0.000002	+0.000343	0.000733

TABLE IV. VALUES FOR $J'_n(x)$

n \ x	5.3	5.4	5.5	8.1	8.6
0	+0.345961	+0.345345	0.341438	-0.247608	-0.272755
1	-0.010527	+0.022743	+0.055236	+0.116949	-0.017093
2	-0.325301	-0.313235	-0.298778	+0.268936	+0.261404
3	-0.227187	-0.242876	-0.257016	-0.021126	+0.136036
4	+0.003037	-0.014472	-0.032403	-0.226743	-0.146209
5	+0.117959	+0.111955	+0.104967	-0.229385	-0.247895
6	+0.113237	+0.115463	+0.117162	-0.081326	-0.147769
7	+0.068491	+0.072552	+0.076563	+0.048520	-0.002512
8	+0.031752	+0.034635	+0.037646	+0.095652	+0.079718
9	+0.012142	+0.013588	+0.015151	+0.083578	+0.090781
10	+0.003983	+0.004563	+0.005208	+0.053158	+0.066855
11	+0.001148	+0.001345	+0.001570	+0.027574	+0.038738
12	+0.000296	+0.000354	+0.000423	+0.012262	+0.018930
13	+0.000069	+0.000085	+0.000103	+0.004808	+0.008083
14	+0.000015	+0.000018	+0.000023	+0.001693	+0.003082
15	+0.000003	+0.000004	+0.000005	+0.000542	+0.001066

TABLE V. VALUES FOR $Y_n(x)$

n \ x	5.3	5.4	5.5	8.1	8.6
0	-0.337437	-0.340168	-0.339481	+0.238091	+0.271458
1	+0.044548	+0.010127	-0.023758	-0.133149	+0.001084
2	+0.354248	+0.343919	+0.330841	-0.270968	-0.271206
3	+0.222809	+0.244627	+0.264370	-0.000662	-0.127226
4	-0.102011	-0.072111	-0.042438	+0.270477	+0.182443
5	-0.376788	-0.351458	-0.326098	+0.267800	+0.296941
6	-0.608910	-0.578737	-0.550467	+0.060140	+0.162837
7	-1.001876	-0.934625	-0.874921	-0.178703	-0.069727
8	-2.037554	-1.844365	-1.676605	-0.369010	-0.276345
9	-5.149231	-4.530160	-4.002476	-0.550206	-0.444404
10	-15.450402	-13.256168	-11.422406	-0.853669	-0.653803
11	-53.154171	-44.566760	-37.533547	-1.557619	-1.076068
12	-205.189552	-168.312112	-138.711781	-3.376901	-2.078928
13	-876.006063	-703.487069	-567.754225	-8.448014	-4.781406
14	-4092.198680	-3218.847850	-2545.217281	-23.740180	-12.356486
15	-20743.15677	-15986.83511	-12389.71557	-73.616806	-35.449012

TABLE VI. VALUES FOR $Y'_n(x)$

x → / n ↓	5.3	5.4	5.5	8.1	8.6
0	-0.044548	-0.010127	+0.023758	+0.133149	-0.001084
1	-0.345843	-0.342043	-0.335161	+0.254529	+0.271332
2	-0.089131	-0.117250	-0.144064	-0.066243	+0.064155
3	+0.228129	+0.208015	+0.186639	-0.270722	-0.226824
4	+0.299799	+0.298043	+0.295234	-0.134231	-0.212083
5	+0.253449	+0.253313	+0.254015	+0.105168	+0.009803
6	+0.312544	+0.291584	+0.274412	+0.223252	+0.183334
7	+0.714322	+0.632814	+0.563069	+0.214575	+0.219591
8	+2.073678	+1.797767	+1.563777	+0.185751	+0.187339
9	+6.706424	+5.705902	+4.872901	+0.242329	+0.188729
10	+24.002470	+20.018300	+16.765536	+0.503707	+0.315832
11	+94.869575	+77.527972	+63.644687	+1.261616	+0.722563
12	+411.425946	+329.460152	+265.110339	+3.445197	+1.852669
13	+1943.504564	+1525.267869	+1203.252750	+10.181640	+5.128779
14	+9933.575355	+7641.674020	+5910.980675	+32.584396	+15.333803
15	+54614.84878	+41189.02745	+31244.91609	112.587239	+49.473186

REFERENCES

1. E. C. Jordan, Electromagnetic Waves and Radiating Systems, Prentice-Hall, Inc., New York, 1951, pp. 593-597.
2. J. R. Wait, Electromagnetic Radiation from Cylindrical Structures, Pergamon Press, New York, 1959, pp. 133-135.
3. W. V. T. Rusch, Radiation from a Plasma-clad Axially-slotted Cylinder, USCEC Report 82-201, University of Southern California, School of Engineering, May 1962.
4. H. Hodara and G. I. Cohn, "Radiation from a Gyro-Plasma Coated Magnetic Line Source," IRE Transactions on Antennas and Propagation, Vol. AP-10, No. 5, September, 1962, pp. 581-593.
5. Samuel Silver and William K. Saunders, "The External Field Produced by a Slot in an Infinite Circular Cylinder," Journal of Applied Physics, Vol. 21, Feb., 1950, pp. 153-158.
6. Samuel Silver and William K. Saunders, "The Radiation from a Transverse Slot in a Circular Cylinder," Journal of Applied Physics, Vol. 21, Aug. 1950, pp. 745-749.
7. V. L. Ginzburg, Propagation of Electromagnetic Waves in Plasma, Gordon and Breach Science Publishers, Inc., New York, 1961.
8. Lyman Spitzer, Physics of Fully Ionized Gases, Interscience Publishers, Inc., New York, 1956, pp. 50-51.
9. G. N. Watson, The Theory of Bessel Functions, The University Press, Cambridge, England, 1952.

DISTRIBUTION LIST

Copy No.	Addressee
1-10	Commander Armed Services Technical Information Agency Arlington Hall Station Arlington 12, Virginia ATTN: TIPRD
11-17	Commander Aeronautical Systems Division Wright-Patterson Air Force Base, Ohio
(11-12)	ATTN: ASAPRD
(13)	ATTN: ASAPT
(14-15, 1 repro.)	ATTN: ASRNGE-1
(16)	ATTN: ASNVEB
(17)	ATTN: ASNRD
18	Aerospace Corporation P. O. Box 95085 Los Angeles 45, California ATTN: D. A. Lacer
19	Giannini Research Laboratory 3841 S. Main Street Santa Ana, California ATTN: Elmer Vecchio
20	Carlyle Barton Laboratory The Johns Hopkins University Charles and 34th Sts. Baltimore 18, Maryland ATTN: Mr. John M. Kopper
21	Commanding Officer, Space Systems Division, SSPI AF Unit Post Office Los Angeles 45, California ATTN: Capt. S. R. Townsend
22	Headquarters, USAF The Pentagon, Washington 25, D. C. ATTN: Mr. D. McKanna, AFORT-GW/2
23	Space Systems Division (SAFSP) Air Force Unit Post Office Los Angeles, California ATTN: Capt. Gorman
24	Motorola, Incorporated Military Electronics Division 8201 E. McDowell Road Scottsdale, Arizona ATTN: Mr. Carl A. Helber
25	National Aeronautics and Space Administration Manned Spacecraft Center, Electrical Systems Branch Houston, Texas ATTN: Mr. J. R. McCown
26	Headquarters Research and Technology Division Air Force Systems Command Bolling Air Force Base Washington 25, D. C. ATTN: RTHR
27	Deputy Chief of Staff for Research & Engineering Headquarters, USAF Asst. for Applied Research Washington 25, D. C.
28	Rome Air Development Center Griffiss Air Force Base, New York ATTN: Documents Library, RAALD
29	Commander Air Force Cambridge Research Center 230 Albany Street Cambridge 39, Massachusetts ATTN: Electronic Research Library
30	Space Systems Division (AFSC) Air Force Unit Post Office Los Angeles 45, California ATTN: Library
31	Director, Air University Library Maxwell Air Force Base, Alabama ATTN: AUL-9643
32	Assistant Secretary of Defense Research & Development Board Department of Defense Washington 25, D. C.
33	Secretary, Committee of Electronics Office of Asst. Secretary of Defense Department of Defense Washington 25, D. C.
34	Commanding Officer U. S. Army Signal R & D Laboratory Fort Monmouth, New Jersey ATTN: SIG-RA/SL-RDR
35	Office of the Chief Signal Officer Department of the Army Washington 25, D. C. ATTN: Engineering & Technical Division SIG-RD-5a
36	Chief Bureau of Naval Weapons Department of the Navy Washington 25, D. C. ATTN: Electronics Division
37	Bureau of Naval Weapons Fleet Readiness Central BWFRR Wright-Patterson Air Force Base, Ohio ATTN: Electronics Division
38	Chief, Bureau of Ships Department of the Navy Washington 25, D. C. ATTN: Code 816
39	Director, Naval Research Laboratory Washington 25, D. C. ATTN: Code 2021
40	Commanding Officer U. S. Army Signal R & D Laboratory Fort Monmouth, New Jersey ATTN: SIGRA/SL-SRE Mr. S. J. Grossman
41	Commanding Officer U. S. Army Combat Surveillance Agency 1124 N. Highland Street Arlington 1, Virginia ATTN: Mr. Leonard Plotkin

Copy No.	Addressee
42	Bell Telephone Laboratories Whippany Laboratory Whippany, New Jersey ATTN: Mr. A. C. Price
43	Conductron Corporation 343 South Main Street Ann Arbor, Michigan ATTN: Dr. W. Vivian
44	Goodyear Aircraft Corp. Arizona Division Phoenix, Arizona ATTN: Mr. R. G. LeSage
45	Lockheed Missiles & Space Division 3251 Hanover Street Palo Alto, California ATTN: Tech. Information Center
46	Massachusetts Institute of Technology Electronics Systems Laboratory Cambridge 39, Massachusetts ATTN: Mr. Laurence Swain, Jr.
47	Radio Corporation of America Aerospace Communications & Control Div. Defense Electronics Products Camden 2, New Jersey ATTN: Dr. W. C. Curtis
48	Antenna Laboratory Department of Electrical Engineering The Ohio State University 2024 Neil Avenue Columbus 10, Ohio ATTN: Dr. R. L. Cosgriff
49	Rand Corporation 1700 Main Street Santa Monica, California ATTN: Dr. H. H. Bailey
50	Headquarters, U. S. Army Liaison Group Project MICHIGAN The University of Michigan P. O. Box 618 Ann Arbor, Michigan

AD Div. 8/1

Inst. of Science and Technology, U. of Mich., Ann Arbor
THE RADIATION FIELD PRODUCED BY AN INFINITE SLOT IN AN INFINITE CYLINDER SURROUNDED BY A HOMOGENEOUS PLASMA SHEATH, by Dipak L. Sengupta. May 63. 37 p. incl. illus., tables, 9 refs.
(Report No. 4563-35-T)
(Contract AF 33(616)-8365) Unclassified report

The radiation properties of a slotted cylinderical antenna surrounded by a homogeneous plasma sheath have been investigated. The slot is axial and extends along the entire length of the cylinder; it is fed by a voltage of constant magnitude and phase. The antenna is insulated from the plasma by a thin dielectric coating.

General expressions for the field components are derived, and then simplified by making some physical approximations. The radiation pattern produced by the antenna (over)

UNCLASSIFIED

I. Sengupta, Dipak L.
II. U. S. Air Force
III. Contract AF 33(616)-8365

Armed Services Technical Information Agency
UNCLASSIFIED

AD Div. 8/1

Inst. of Science and Technology, U. of Mich., Ann Arbor
THE RADIATION FIELD PRODUCED BY AN INFINITE SLOT IN AN INFINITE CYLINDER SURROUNDED BY A HOMOGENEOUS PLASMA SHEATH, by Dipak L. Sengupta. May 63. 37 p. incl. illus., tables, 9 refs.
(Report No. 4563-35-T)
(Contract AF 33(616)-8365) Unclassified report

The radiation properties of a slotted cylinderical antenna surrounded by a homogeneous plasma sheath have been investigated. The slot is axial and extends along the entire length of the cylinder; it is fed by a voltage of constant magnitude and phase. The antenna is insulated from the plasma by a thin dielectric coating.

General expressions for the field components are derived, and then simplified by making some physical approximations. The radiation pattern produced by the antenna (over)

UNCLASSIFIED

I. Sengupta, Dipak L.
II. U. S. Air Force
III. Contract AF 33(616)-8365

Armed Services Technical Information Agency
UNCLASSIFIED

AD Div. 8/1

Inst. of Science and Technology, U. of Mich., Ann Arbor
THE RADIATION FIELD PRODUCED BY AN INFINITE SLOT IN AN INFINITE CYLINDER SURROUNDED BY A HOMOGENEOUS PLASMA SHEATH, by Dipak L. Sengupta. May 63. 37 p. incl. illus., tables, 9 refs.
(Report No. 4563-35-T)
(Contract AF 33(616)-8365) Unclassified report

The radiation properties of a slotted cylinderical antenna surrounded by a homogeneous plasma sheath have been investigated. The slot is axial and extends along the entire length of the cylinder; it is fed by a voltage of constant magnitude and phase. The antenna is insulated from the plasma by a thin dielectric coating.

General expressions for the field components are derived, and then simplified by making some physical approximations. The radiation pattern produced by the antenna (over)

UNCLASSIFIED

I. Sengupta, Dipak L.
II. U. S. Air Force
III. Contract AF 33(616)-8365

Armed Services Technical Information Agency
UNCLASSIFIED

AD Div. 8/1

Inst. of Science and Technology, U. of Mich., Ann Arbor
THE RADIATION FIELD PRODUCED BY AN INFINITE SLOT IN AN INFINITE CYLINDER SURROUNDED BY A HOMOGENEOUS PLASMA SHEATH, by Dipak L. Sengupta. May 63. 37 p. incl. illus., tables, 9 refs.
(Report No. 4563-35-T)
(Contract AF 33(616)-8365) Unclassified report

The radiation properties of a slotted cylinderical antenna surrounded by a homogeneous plasma sheath have been investigated. The slot is axial and extends along the entire length of the cylinder; it is fed by a voltage of constant magnitude and phase. The antenna is insulated from the plasma by a thin dielectric coating.

General expressions for the field components are derived, and then simplified by making some physical approximations. The radiation pattern produced by the antenna (over)

UNCLASSIFIED

I. Sengupta, Dipak L.
II. U. S. Air Force
III. Contract AF 33(616)-8365

Armed Services Technical Information Agency
UNCLASSIFIED

AD

are discussed for the following two cases: (i) when both the dielectric coating and the plasma are thin, and (ii) when only the dielectric coating is thin. For both cases field expressions are derived for operating frequency above the plasma frequency and below it. The effects of collision between the particles in the plasma are taken into account. Results for the collisionless case can be obtained from the general expressions given. Numerical results are obtained for the radiation patterns produced by the antenna under various physical situations.

UNCLASSIFIED

DESCRIPTORS

Antennas
Slot antennas
Antenna radiation patterns

UNCLASSIFIED

AD

are discussed for the following two cases: (i) when both the dielectric coating and the plasma are thin, and (ii) when only the dielectric coating is thin. For both cases field expressions are derived for operating frequency above the plasma frequency and below it. The effects of collision between the particles in the plasma are taken into account. Results for the collisionless case can be obtained from the general expressions given. Numerical results are obtained for the radiation patterns produced by the antenna under various physical situations.

UNCLASSIFIED

DESCRIPTORS

Antennas
Slot antennas
Antenna radiation patterns

UNCLASSIFIED

AD

are discussed for the following two cases: (i) when both the dielectric coating and the plasma are thin, and (ii) when only the dielectric coating is thin. For both cases field expressions are derived for operating frequency above the plasma frequency and below it. The effects of collision between the particles in the plasma are taken into account. Results for the collisionless case can be obtained from the general expressions given. Numerical results are obtained for the radiation patterns produced by the antenna under various physical situations.

UNCLASSIFIED

DESCRIPTORS

Antennas
Slot antennas
Antenna radiation patterns

UNCLASSIFIED

AD

are discussed for the following two cases: (i) when both the dielectric coating and the plasma are thin, and (ii) when only the dielectric coating is thin. For both cases field expressions are derived for operating frequency above the plasma frequency and below it. The effects of collision between the particles in the plasma are taken into account. Results for the collisionless case can be obtained from the general expressions given. Numerical results are obtained for the radiation patterns produced by the antenna under various physical situations.

UNCLASSIFIED

DESCRIPTORS

Antennas
Slot antennas
Antenna radiation patterns

UNCLASSIFIED